On the separation of simultaneous-source data by inversion

Gboyega Ayeni, Ali Almomin and Dave Nichols

ABSTRACT

Simultaneous-source data can be adequately separated using an inversion formulation. To recover component shot records, we formulate the data-separation problem as a simultaneous Radon inversion problem. By minimizing the resulting objective function with a robust *hybrid* solver, we obtain high-quality estimates of the component shot records. Furthermore, regularization with directional Laplacians improves the data quality. In our approach, we estimate a single model that predicts all recorded data, and we treat all components of the recorded data as signal. Within limits of operational possibilities, our method can be applied to any number of sources within a single survey and can be easily extended to multiple (time-lapse) surveys. Using 2D sections extracted from the 3D SEAM geophysical model, we show that our method can give results of comparable quality to the original independent shot records.

INTRODUCTION

Conventionally, seismic data acquisition involves a single seismic source and an array of receivers. However, recent advances in acquisition technology enable seismic acquisition with multiple sources (Womack et al., 1990; Hampson et al., 2008; Beasley, 2008). By using simultaneous sources, it is possible to achieve longer offsets, better shot-sampling, and improved time and cost efficiency (van Mastrigt et al., 2002; Berkhout et al., 2008; Howe et al., 2009).

Although direct imaging of simultaneous-source data has several desirable properties, it also suffers from several pitfalls. The most important limitation of direct imaging is the introduction of crosstalk artifacts from incongruous sources. Under certain conditions, crosstalk artifacts may be sufficiently attenuated by stacking (Beasley, 2008; Hampson et al., 2008). Linearized inversion can attenuate crosstalk artifacts significantly (Ayeni et al., 2009; Dai and Schuster, 2009; Tang and Biondi, 2009). However, linearized inversion assumes that the true seismic velocities are known, which is not the case in any practical application. Therefore, most practitioners opt to separate simultaneous-source data sets into independent shot records followed by conventional processing.

Data separation may be treated as a filtering (Moore et al., 2008; Huo et al., 2009) or an inversion (Akerberg et al., 2008; Abma et al., 2010) problem. In this paper, we

take an inversion approach, in which components of the simultaneous-source data are predictable from a single model. In our formulation, the simultaneous-source data are modeled by a composite Radon operator based on the recording geometries and relative shot times of the simultaneous sources. We solve the resulting regression using a robust *hybrid*-norm solver (Li et al., 2010). Model sparsity, introduced by the *hybrid*-norm, significantly improves the quality of the recovered data sets relative to those from an l_2 solver.

The quality of the separated data is further improved by introducing model regularization, which may be implemented in either the Radon or the shot space. In this paper, for the single-survey problem, we consider regularization by damping and by directional Laplacians (Hale, 2007). In our problem, non-stationary directional Laplacians are used to enforce smoothness along local dips. First, we solve the inversion problem using a damping regularization. Then, using the estimated independent data, we compute dip-components along constant-offset panels. From these dip estimates, regularization operators for the next inversion step are generated. These operators are used to regularize the inversion and generate new results that serve as inputs to the next inversion step. This procedure can be repeated as many times as necessary.

One potential application of simultaneous-source acquisition is in time-lapse seismic reservoir monitoring (Ayeni et al., 2009). For example, because this method reduces seismic acquisition cost, monitoring data sets can be acquired at shorter time intervals. However, because time-lapse monitoring requires high-quality data, amplitudes of separated data must be reliable. For the time-lapse seismic problem, we consider a spatio-temporal regularization scheme that utilizes a combination of directional Laplacians and temporal smoothness constraints.

In this paper, we first describe the inversion formulation of our separation approach. Next, we briefly discuss possible regularization schemes for this inversion problem. Finally, using data sets from 2D sections extracted from the SEAM geophysical model, we show that our method can produce high-quality results for both single and time-lapse surveys.

METHOD

We can represent the simultaneous-source acquisition process for n sources as follows:

$$\sum_{i=1}^{n} \mathbf{S}\mathbf{d}_i = \mathbf{d}, \tag{1}$$

where $\mathbf{S}$ is a shifting operator built from the relative time-delays between sources, $\mathbf{d}_i$ is the data due to source i, and $\mathbf{d}$ is the simultaneous-source data. We can rewrite this equation in the form

$$\top\mathbf{H}_i\mathbf{m} \approx \mathbf{d}, \tag{2}$$

where $\top$ is the summation operator, and $\mathbf{H}_i$ is an operator that models data $\mathbf{d}_i$ from model $\mathbf{m}$. Note here, that all component shots of the encoded data $\mathbf{d}$ are modeled from a single, consistent model $\mathbf{m}$. In this paper, $\mathbf{H}_i$ is a modified hyperbolic Radon operator that maps data from the the velocity-CMP space to shot-offset space, honoring the time delays at source i relative to a reference shot. Adding a regularization operator $\mathbf{A}$, we have

$$\begin{aligned} \top\mathbf{H}_i\mathbf{m} &\approx \mathbf{d}, \\ \epsilon\mathbf{A}\mathbf{m} &\approx \mathbf{0}, \end{aligned} \tag{3}$$

where ϵ, regularization parameter determines the regularization strength.

There are many possible choices for the regularization operator $\mathbf{A}$. Taking $\mathbf{A}$ to be an identity matrix and minimizing the regressions in equation 3 with a *hybrid* solver leads to a sparse Radon inversion problem. Alternatively, we can regularize the problem with a shot-space operator $\mathbf{B}_i$ by re-writing equation 3 as follows:

$$\begin{aligned} \top\mathbf{H}_i\mathbf{m} &\approx \mathbf{d}, \\ \epsilon\mathbf{B}_i\mathbf{H}_i\mathbf{m} &\approx \mathbf{0}, \end{aligned} \tag{4}$$

which in matrix form can written as

$$\begin{bmatrix} \top \\ \epsilon\mathbf{B}_i \end{bmatrix} \mathbf{H}_i\mathbf{m} \approx \begin{bmatrix} \mathbf{d} \\ \mathbf{0} \end{bmatrix}. \tag{5}$$

In this paper, we define $\mathbf{B}$ as a system of non-stationary dip-filters. First, we compute local event dips using the plane-wave destruction method (Fomel, 2002), then we compute dip-filters using factorized directional Laplacians (Hale, 2007). Because of the random delays between simultaneous sources, for any given source, events from other sources are random in its corresponding common-offset gathers. By destroying predictable events corresponding to source i, operator $\mathbf{B}_i$ ensures that only these events are allowed in the final separated data sets, whereas unpredictable events are not. Events that are not predictable by $\mathbf{B}_i$ are passed on to other sources, where they are predictable by the corresponding operator $\mathbf{B}_j$. We call this inversion method dip-constrained sparse inversion (DCSI). In this paper, we refer to solution of equation 5, with $\mathbf{B}_i$ as an identity matrix, as unconstrained sparse inversion.

However, because the operator $\mathbf{B}_i$ is a function of the separated data, the problem becomes non-linear. To linearize this problem, we start by solving the equation 3 to get an initial estimate for $\mathbf{d}_i$. Then, using $\mathbf{d}_i$, we obtain an estimate of the operator $\mathbf{B}_i$, which is used to regularize the problem starting from initial model estimate $\mathbf{m}$. Results from this new step can then serve as inputs into the next inversion step. This process can be repeated as as many times as necessary.

Following the approach of Abma et al. (2010), instead of using $\mathbf{B}_i$ as a regularization operator, we can use $\mathbf{B}_i^{-1}$ as a smoothing operator by re-writing equation 4 as follows:

$$\begin{aligned} \top\mathbf{B}_i^{-1}\mathbf{H}_i\mathbf{m} &\approx \mathbf{d}, \\ \epsilon\mathbf{I}\mathbf{m} &\approx \mathbf{0}. \end{aligned} \tag{6}$$

In this paper, we implement $\mathbf{B}_i^{-1}$ as polynomial division (Claerbout and Fomel, 2008) with non-stationary directional Laplacians.

Equation 5 can be directly extended to multiple surveys. For example, for two surveys, we can minimize the regressions

$$\begin{aligned}
\begin{bmatrix} \top_1 \\ \epsilon\mathbf{B}_{i1} \end{bmatrix} \mathbf{H}_{i1}\mathbf{m}_1 &\approx \begin{bmatrix} \mathbf{d}_1 \\ \mathbf{0} \end{bmatrix}, \\
\begin{bmatrix} \top_2 \\ \epsilon\mathbf{B}_{i2} \end{bmatrix} \mathbf{H}_{i2}\mathbf{m}_2 &\approx \begin{bmatrix} \mathbf{d}_2 \\ \mathbf{0} \end{bmatrix}, \\
\begin{bmatrix} \lambda\mathbf{Z}_1\mathbf{m}_1 & -\lambda\mathbf{Z}_2\mathbf{S}_{1,2}\mathbf{m}_2 \end{bmatrix} &\approx \mathbf{0},
\end{aligned} \tag{7}$$

where for survey k, $\mathbf{H}_{ik}$ and $\mathbf{B}_{ik}$ are the modeling and shot-space regularization operators, respectively, for source i; $\mathbf{m}_k$ and $\mathbf{d}_k$ are the Radon model and simultaneous-source data; $\mathbf{Z}_k$ is a temporal regularization operator; and $\mathbf{S}_{k,k+1}$ is a shifting operator that aligns the models $\mathbf{m}_k$ and $\mathbf{m}_{k+1}$. Note that $\mathbf{H}_{ik}$ incorporates both geometry and relative shot timing for survey k. Because of differences in geometry and relative shot timing between surveys, operator $\mathbf{H}_{i1}$ is different from $\mathbf{H}_{i2}$. The last regression in equation 7 minimizes the difference between models $\mathbf{m}_1$ and $\mathbf{m}_2$. Because we are interested only in production-related differences between $\mathbf{m}_1$ and $\mathbf{m}_2$, the difference between the two models is also very sparse. We can generalize equation 7 to an arbitrary number of surveys as follows:

$$\begin{aligned}
\begin{bmatrix} \top_k \\ \epsilon\mathbf{B}_{ik} \end{bmatrix} \mathbf{H}_{ik}\mathbf{m}_k &\approx \begin{bmatrix} \mathbf{d}_k \\ \mathbf{0} \end{bmatrix}, \\
\begin{bmatrix} \lambda\mathbf{Z}_k\mathbf{m}_k & -\lambda\mathbf{Z}_{k+1}\mathbf{S}_{k,k+1}\mathbf{m}_{k+1} \end{bmatrix} &\approx \mathbf{0}.
\end{aligned} \tag{8}$$

In this paper, we refer to the method of solving the joint-inversion problem represented by equation 8 as spatio-temporal constrained sparse inversion (STCSI).

EXAMPLES

Using 2D models extracted from the 3D SEAM geophysical model (Figure 1), we consider data separation for three possible simultaneous-source applications. The grids in both models have been modified. All data were modeled with a 2D Acoustic finite-difference algorithm. In each example, we use the different formulations to solve the separation problem described above. All sparse inversion examples are generated using a *hybrid* solver (Li et al., 2010).

Example 1: Separation of complex data sets

In this example, we consider data from a complex 2D salt model (Figure 1(a)). The simultaneous-source data comprise 330 shot gathers from two sources separated by

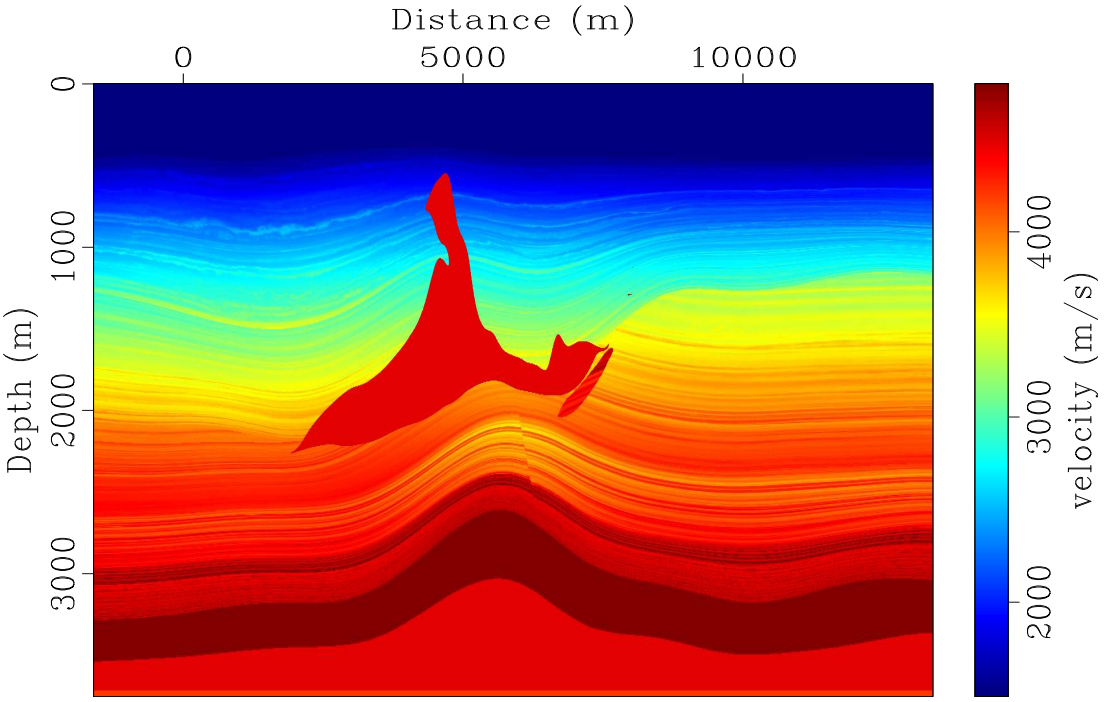

(a)

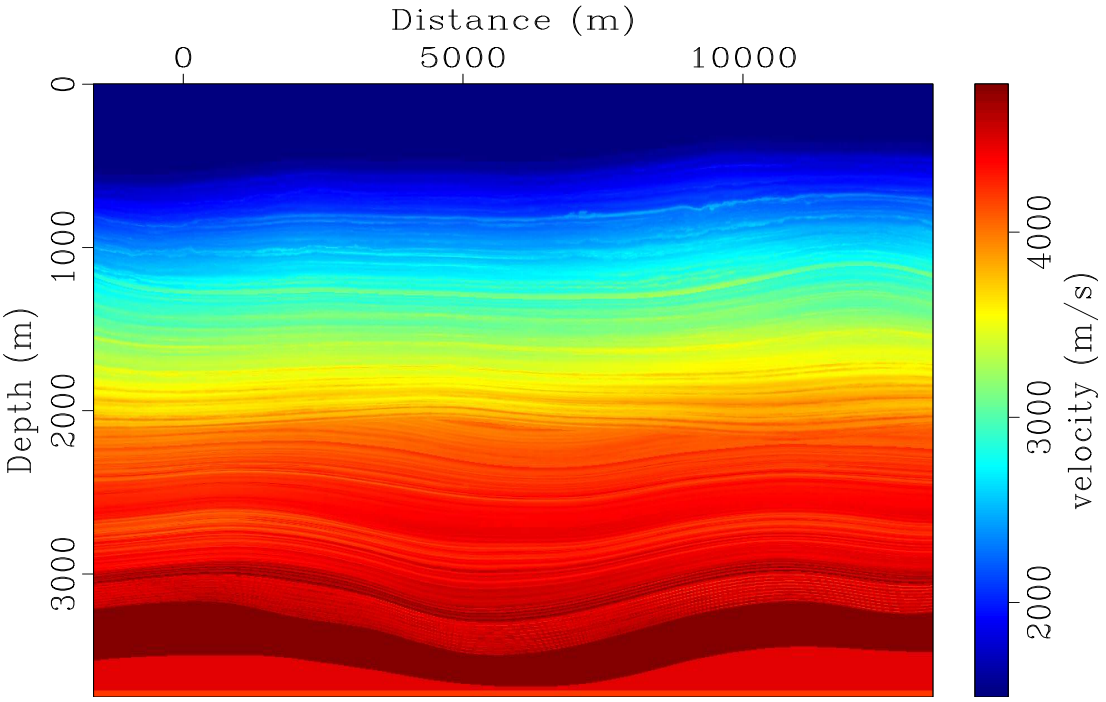

(b)

Figure 1: 2D velocity models extracted from the 3D SEAM geophysical model. [**ER**]

2400 m (Figure 2). This example represents the case where a front seismic vessel is pulling the streamer, and a second boat shoots from the end of the streamer cable—with both sources moving from left to right over the model in Figure 1(a). Note the randomness of data corresponding to the unaligned source in the common-offset plane. The single-source records are shown in Figure 3. The separated data sets recovered by l_2 (conjugate-gradient) inversion are shown in Figure 4. Comparing these results to the single-source data (Figure 3), we see that there are numerous *crosstalk* artifacts in each of the two sources. Separation results obtained by sparse inversion of the data without and with regularization by directional Laplacians are shown in Figures 5 and 6, respectively. Note that in both inversion results, the data are well separated into the component shot records. The residual artifacts present in the unconstrained sparse-inversion results (Figure 5) have been attenuated by regularization (Figure 6). Dips estimated from the unconstrained results (Figure 5) and used to obtain the dip-constrained results (Figure 6) are shown in Figure 7.

Example 2: Separation of multiple sources

In this example, we consider data from the model in Figure 1(b). The simultaneous-source data comprise of data from four sources with 800 m separation (Figure 8). The individual source records are shown in Figure 9. Separation results obtained by inverting the data without dip constraint are shown in Figure 10. Results obtained using the reformulated regressions in equation 6 are shown in Figure 11. Note that residual artifacts seen in the unconstrained results (Figure 10) have been attenuated. Dips estimated from the unconstrained results and used to obtain the constrained results are shown in Figure 12.

Example 3: Joint inversion of simultaneous-source time-lapse data

In this example, we consider conduct a repeatability test on two different data sets from the same model (Figure1(b)). This represents a repeatability test for a time-lapse seismic monitoring case, where only amplitude differences from production-related changes are of interest. We modeled two sets of simultaneous-source data, each comprised of two sources with 2400 m separation (Figure 13). Because it is impractical to repeat both the geometry and relative shooting times between surveys, time-lapse data acquired with simultaneous sources will have high non-repeatability. Therefore, our data separation procedure serves the dual purpose of separating each simultaneous-source data into component shot records and cross-equalizing the time-lapse data sets. The individual source records for each survey are shown in Figure 14.

In this example, because we assume no change in the reservoir between surveys, the difference between the two sets of data is zero (Figures 14(e) and 14(f)). Separation results obtained by inverting the data sets separately without spatio-temporal con-

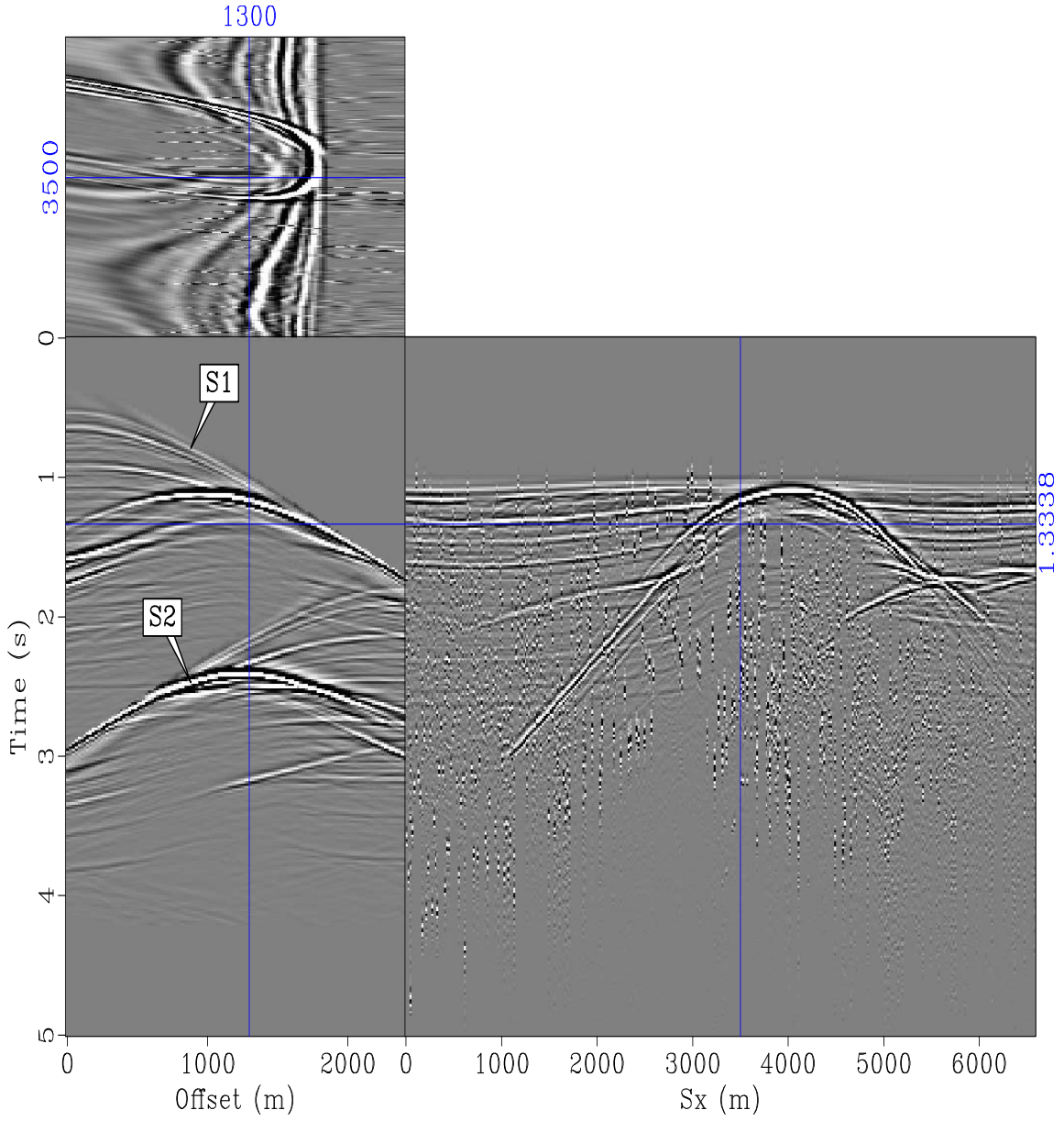

Figure 2: Simultaneous-source data comprising shot-records from two end-on sources (S1 and S2) over the model in Figure 1(a). In this and subsequent figures, the second dimension is offset, and the third dimension is shot position. Note that along the common-offset axis, because the shot times have been referenced to source S1, data corresponding to this source are aligned, whereas those corresponding to S2 are not aligned. [**ER**]

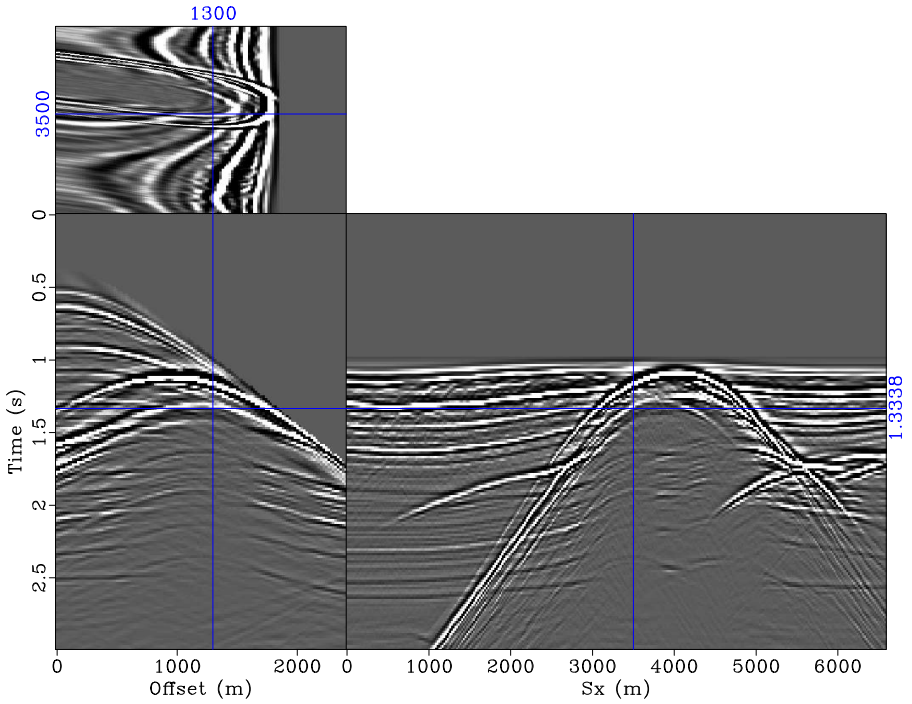

(a)

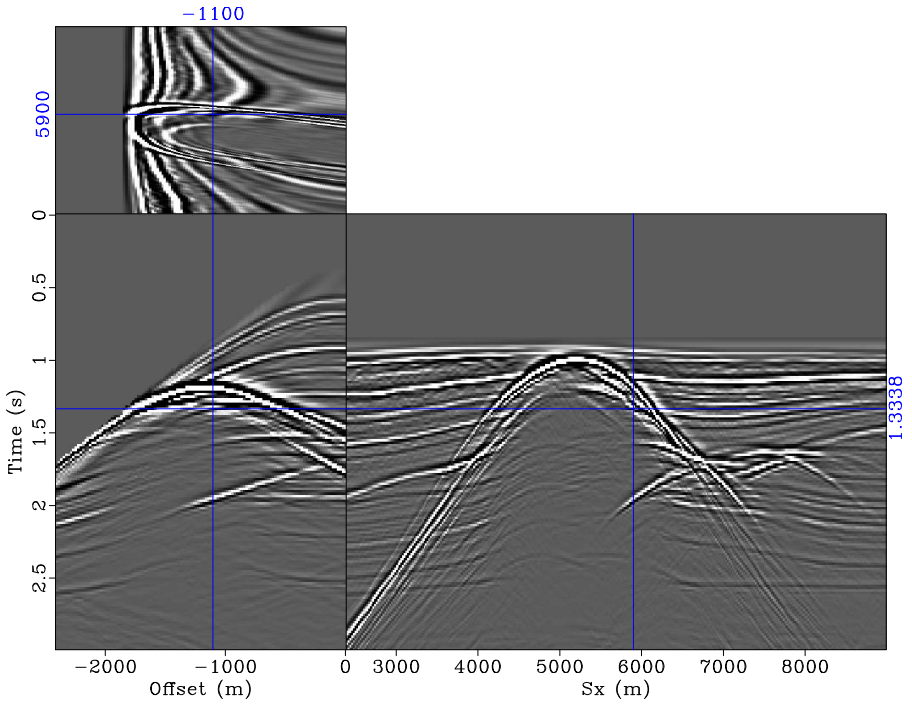

(b)

Figure 3: Single-source data that would have been recorded by (a) source 1 and (b) source 2 over the model in Figure 1(a). These two shot records are the components of the data shown in Figure 2. [**CR**]

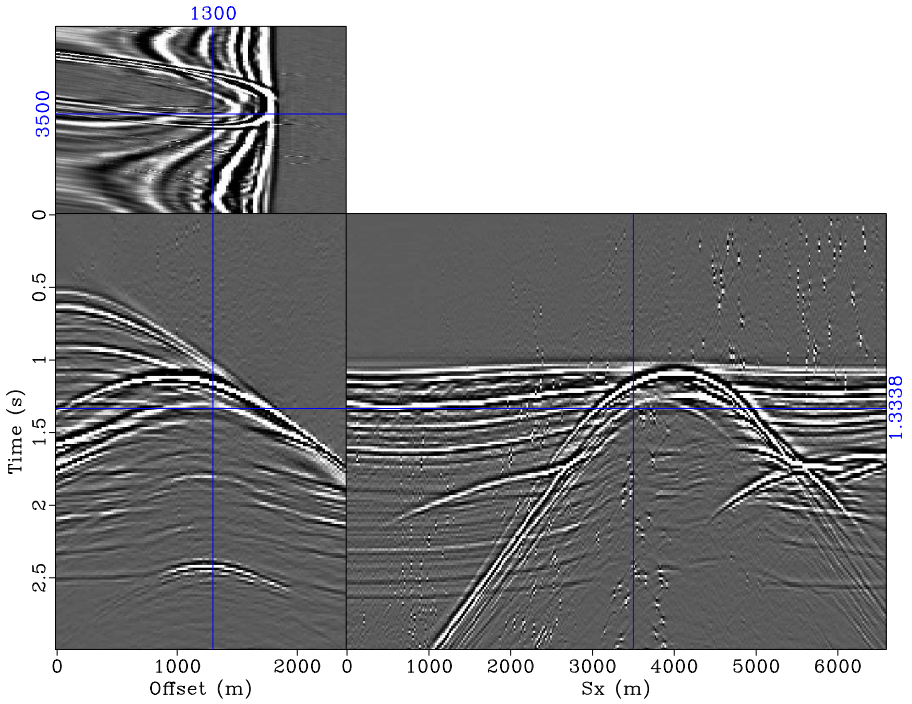

(a)

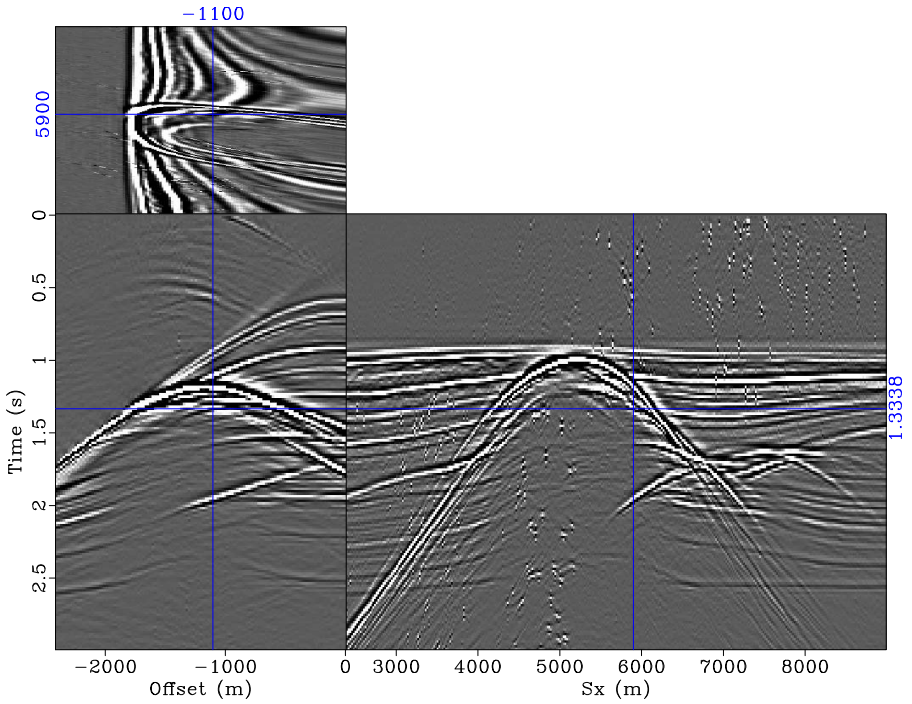

(b)

Figure 4: Shot gathers recovered by unconstrained l_2 inversion for (a) source 1 and (b) source 2. Note that the two data sets are not well separated, as several events which do not exist in the single-source data (Figure 3) are present. [**CR**]

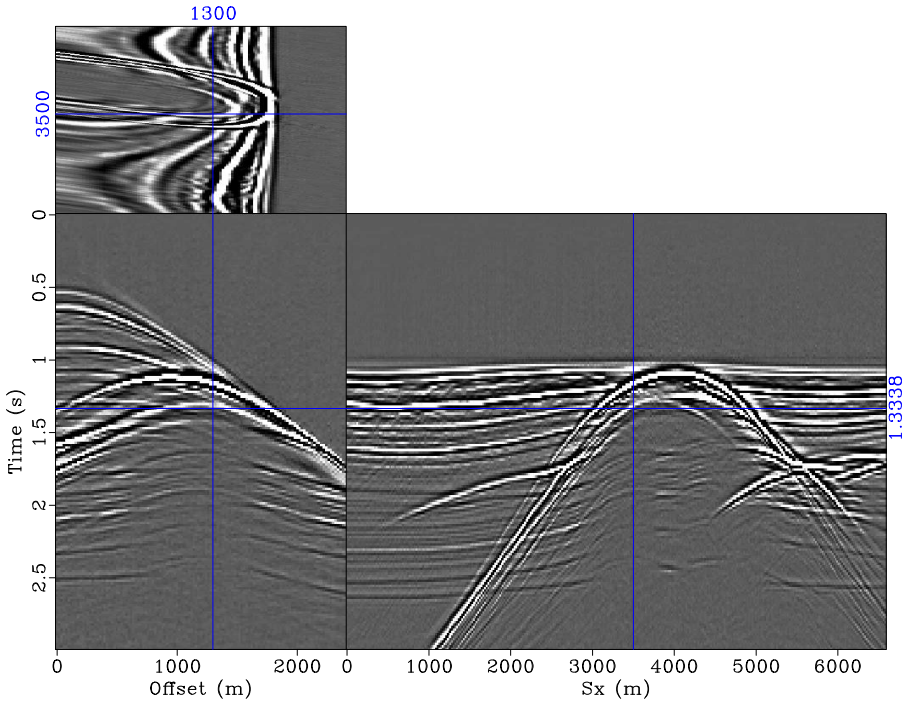

(a)

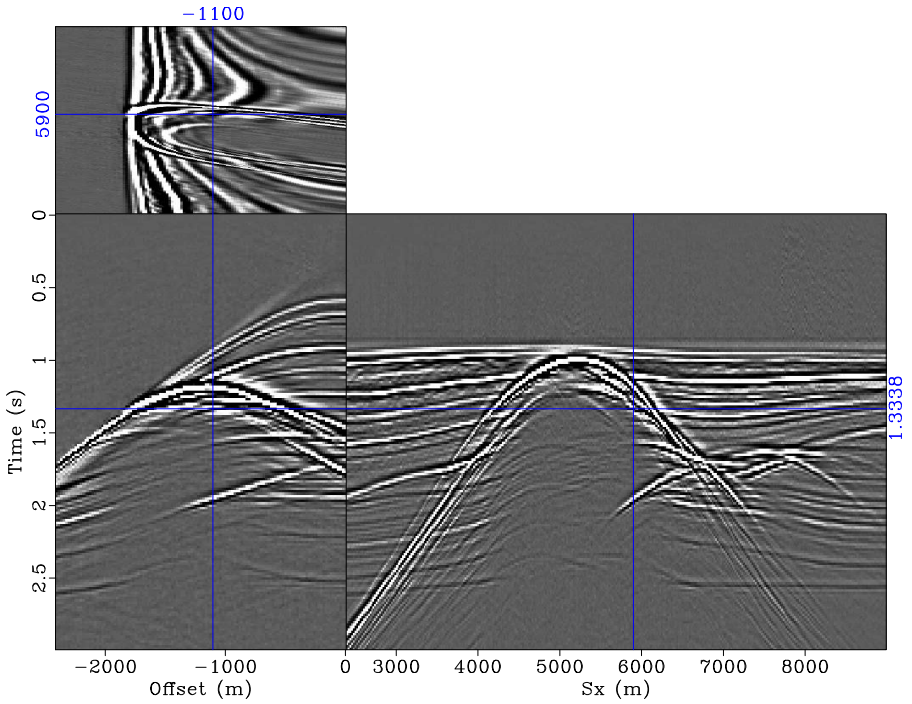

(b)

Figure 5: Shot gathers recovered by unconstrained sparse inversion for (a) source 1 and (b) source 2. Note that the two data sets are well separated and are comparable to the original data (Figure 3). [**CR**]

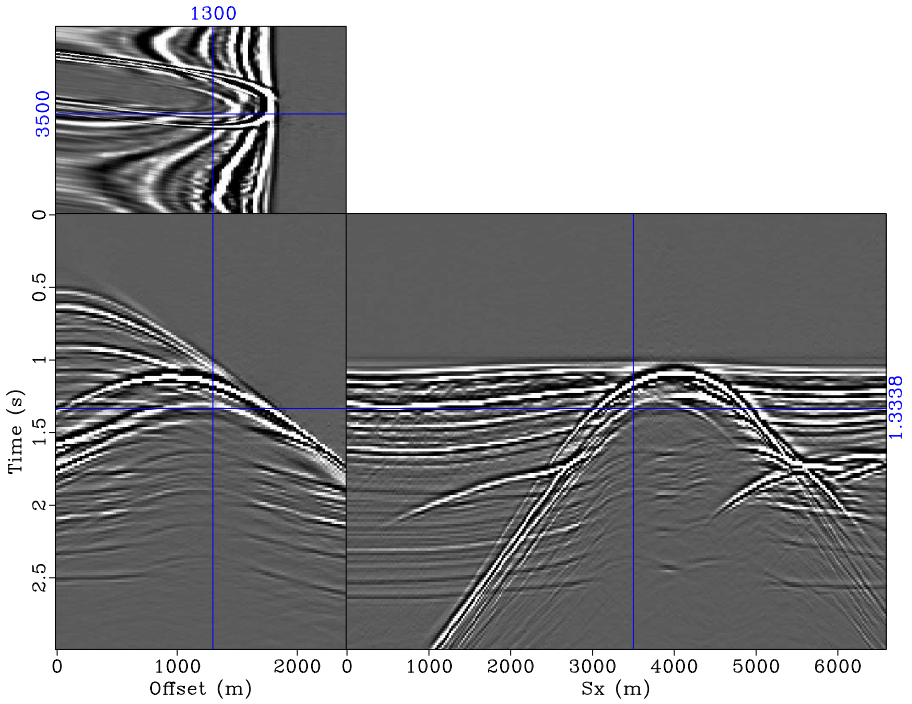

(a)

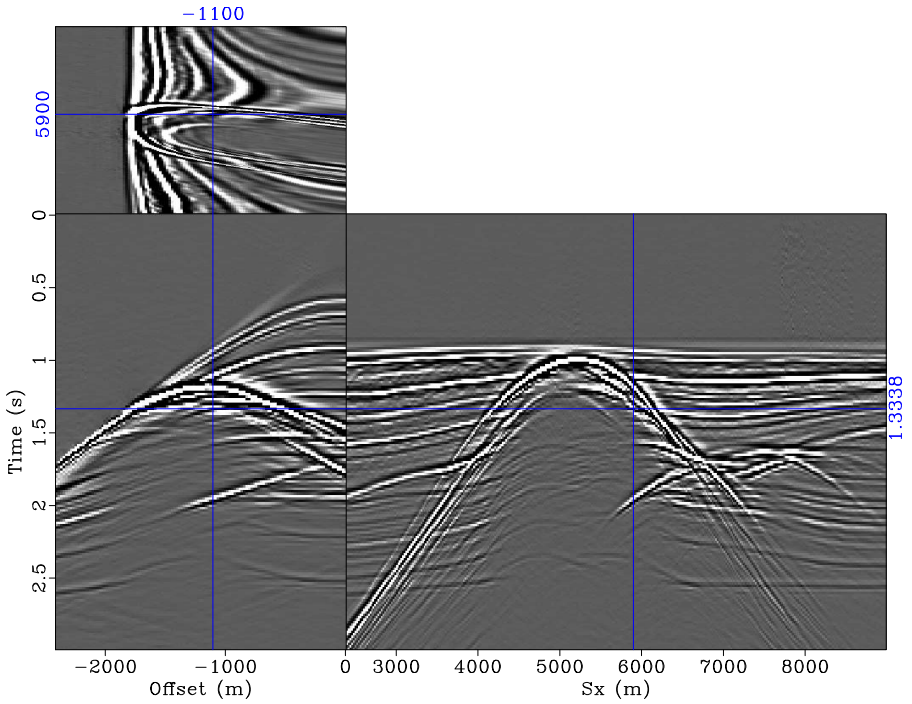

(b)

Figure 6: Shot gathers recovered by dip-constrained sparse inversion for (a) source 1 and (b) source 2. Note that with regularization the residual artifacts present in the unconstrained example (Figure 5) have been attenuated. [**CR**]

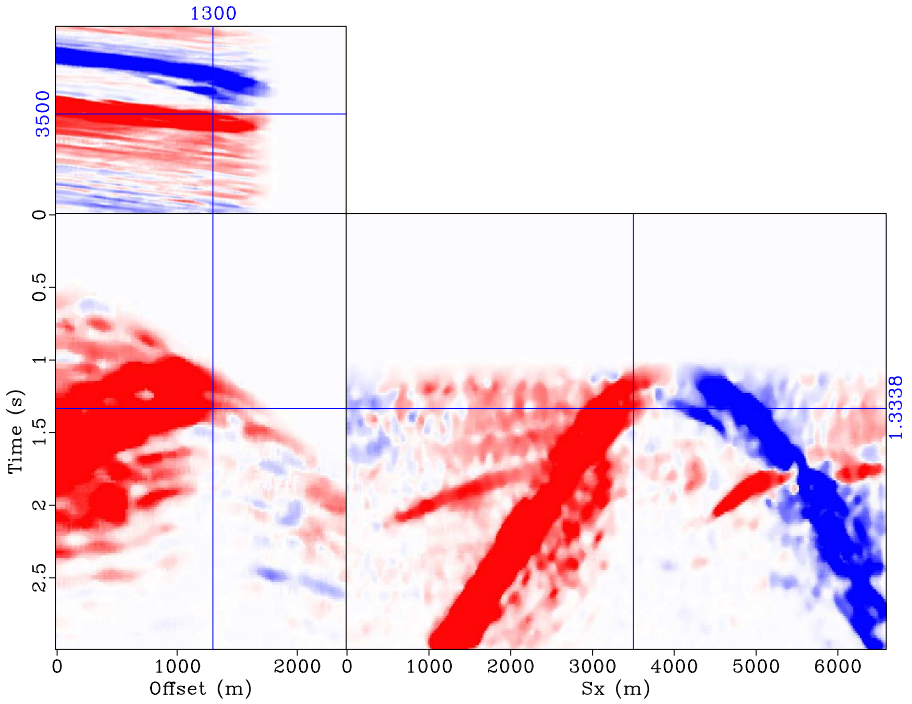

(a)

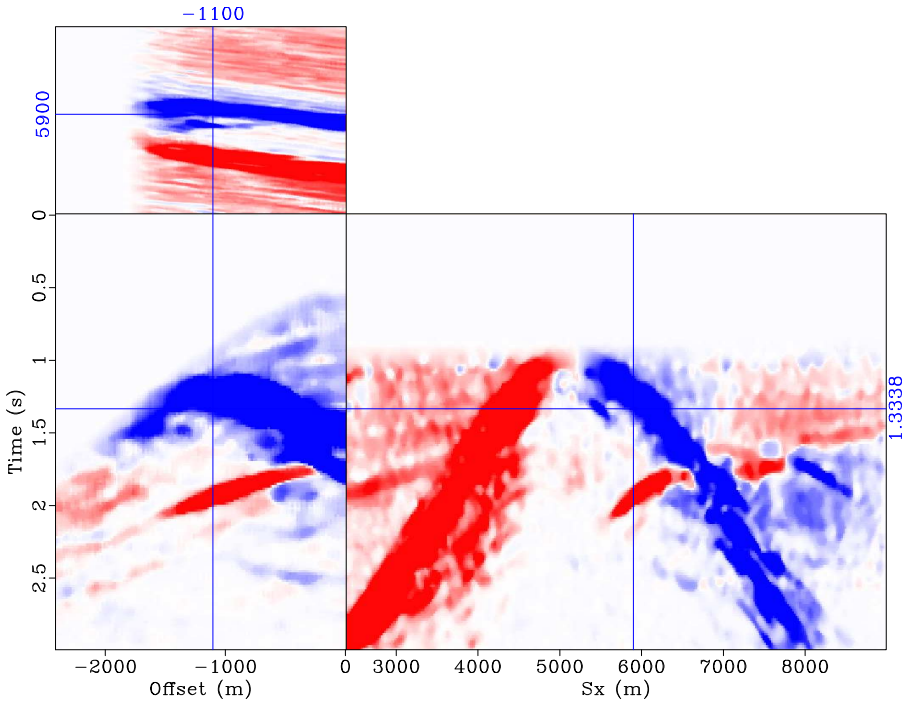

(b)

Figure 7: Local dips (common-offset components) for (a) source 1 and (b) source 2, obtained from the unconstrained sparse inversion (Figure 5) and used in the dip-constrained sparse inversion to obtain the results in Figure 6. [**CR**]

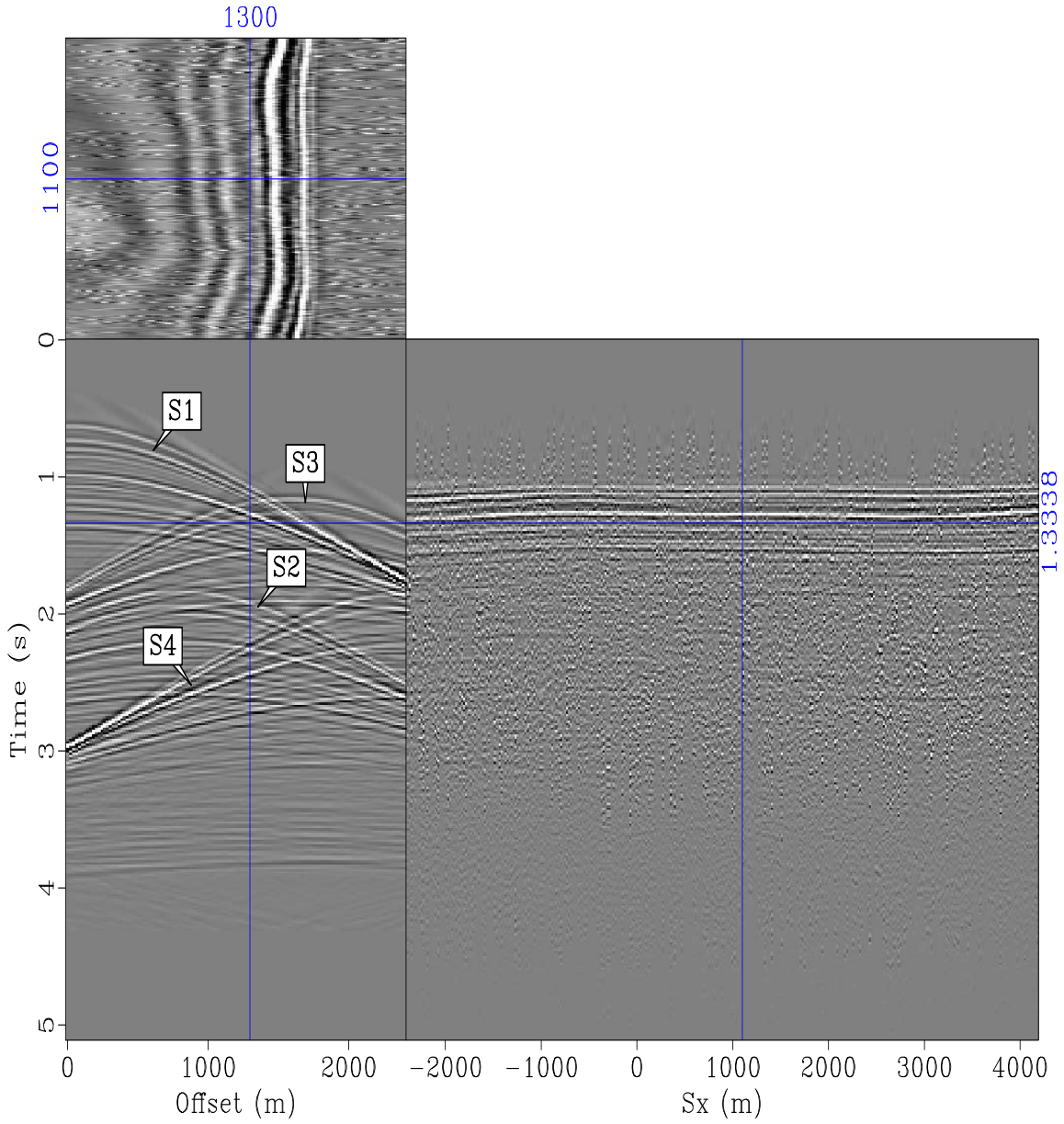

Figure 8: Simultaneous-source data comprising shot-records from four sources (S1, S2, S3 and S4) over the model in Figure 1(b). [**CR**]

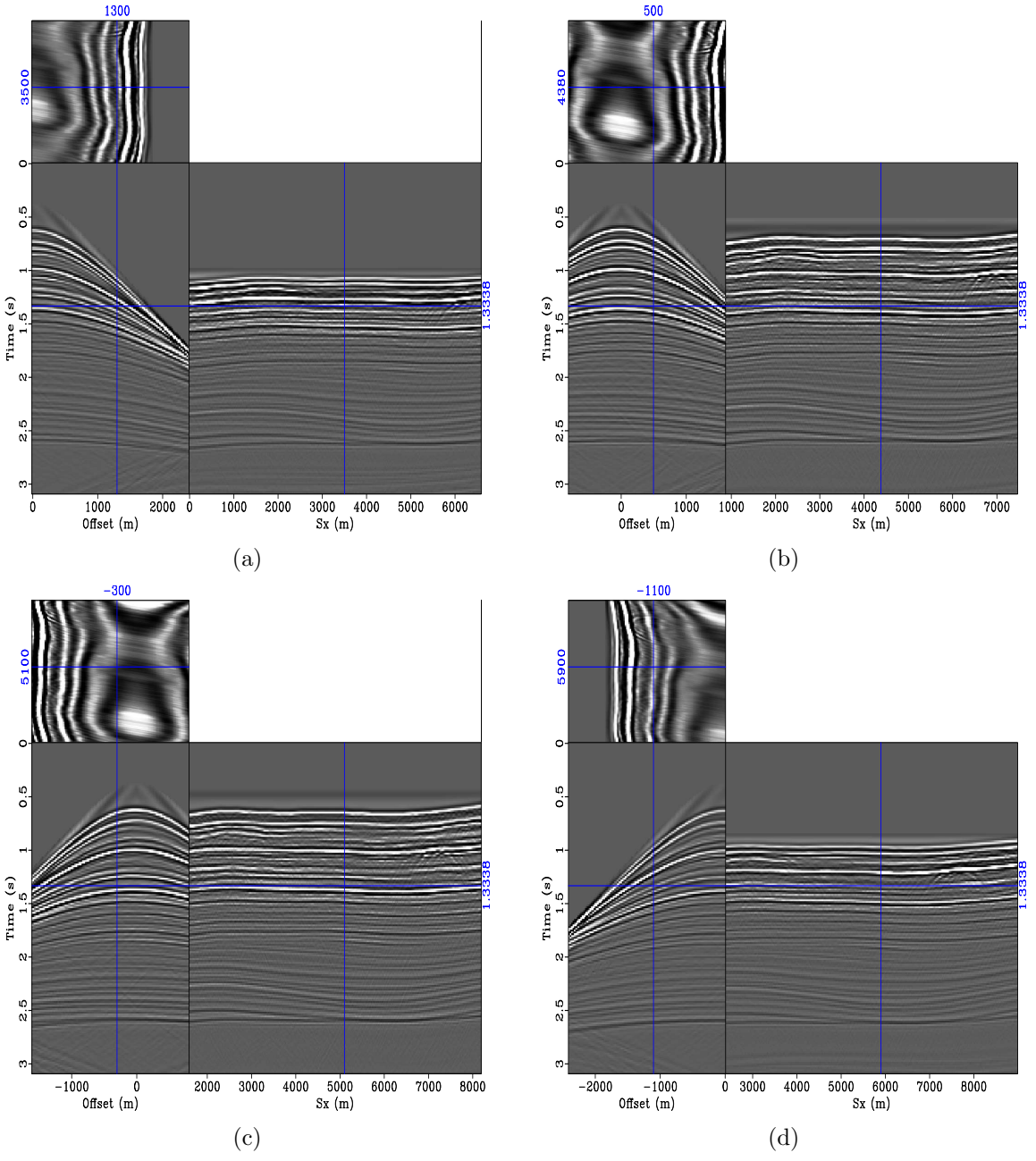

Figure 9: Single-source data that would have been recorded by (a) source 1, (b) source 2, (c) source 3, and (d) source 4 over the model in Figure 1(b). These shot records are the components of the data shown in Figure 8. [**CR**]

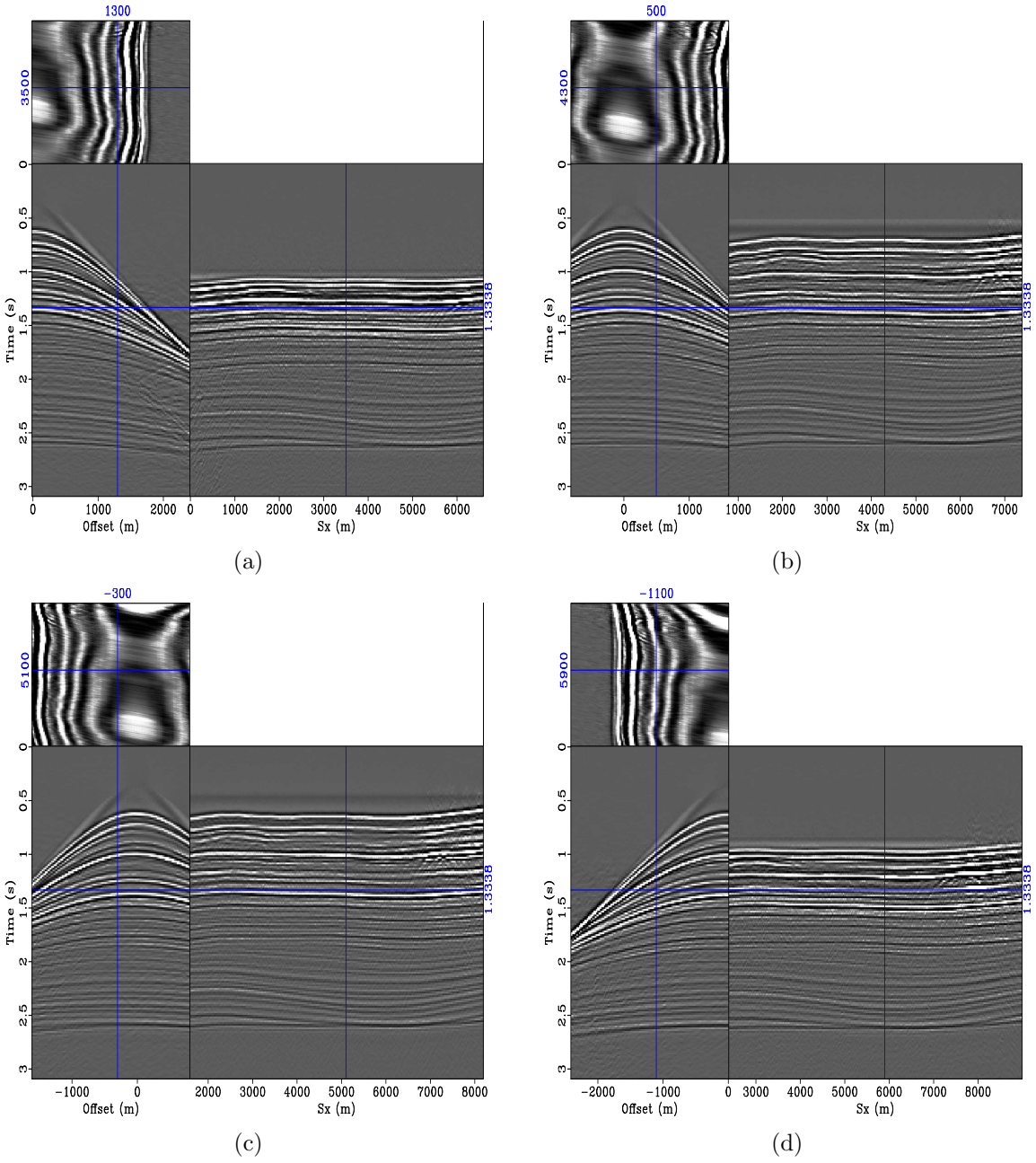

Figure 10: Shot gathers recovered by unconstrained sparse inversion for (a) source 1, (b) source 2, (c) source 3, and (d) source 4. Note that these results contain several residual artifacts compared to the reference single-source records (Figure 9). [**CR**]

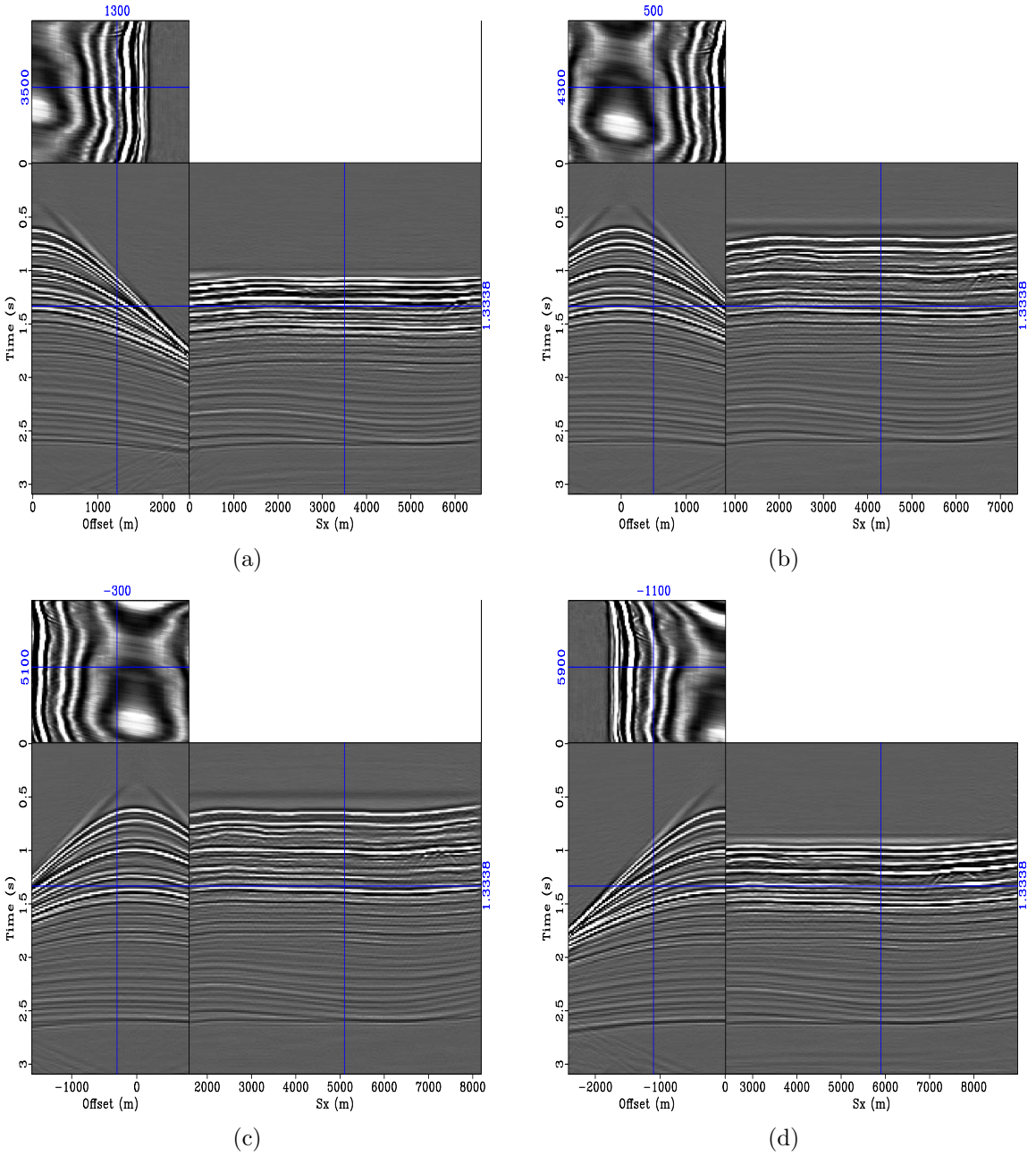

Figure 11: Shot gathers recovered by dip-constrained sparse inversion for (a) source 1, (b) source 2, (c) source 3, and (d) source 4. Residual artifacts present in the unconstrained example (Figure 10) have been attenuated by DCSI. [**CR**]

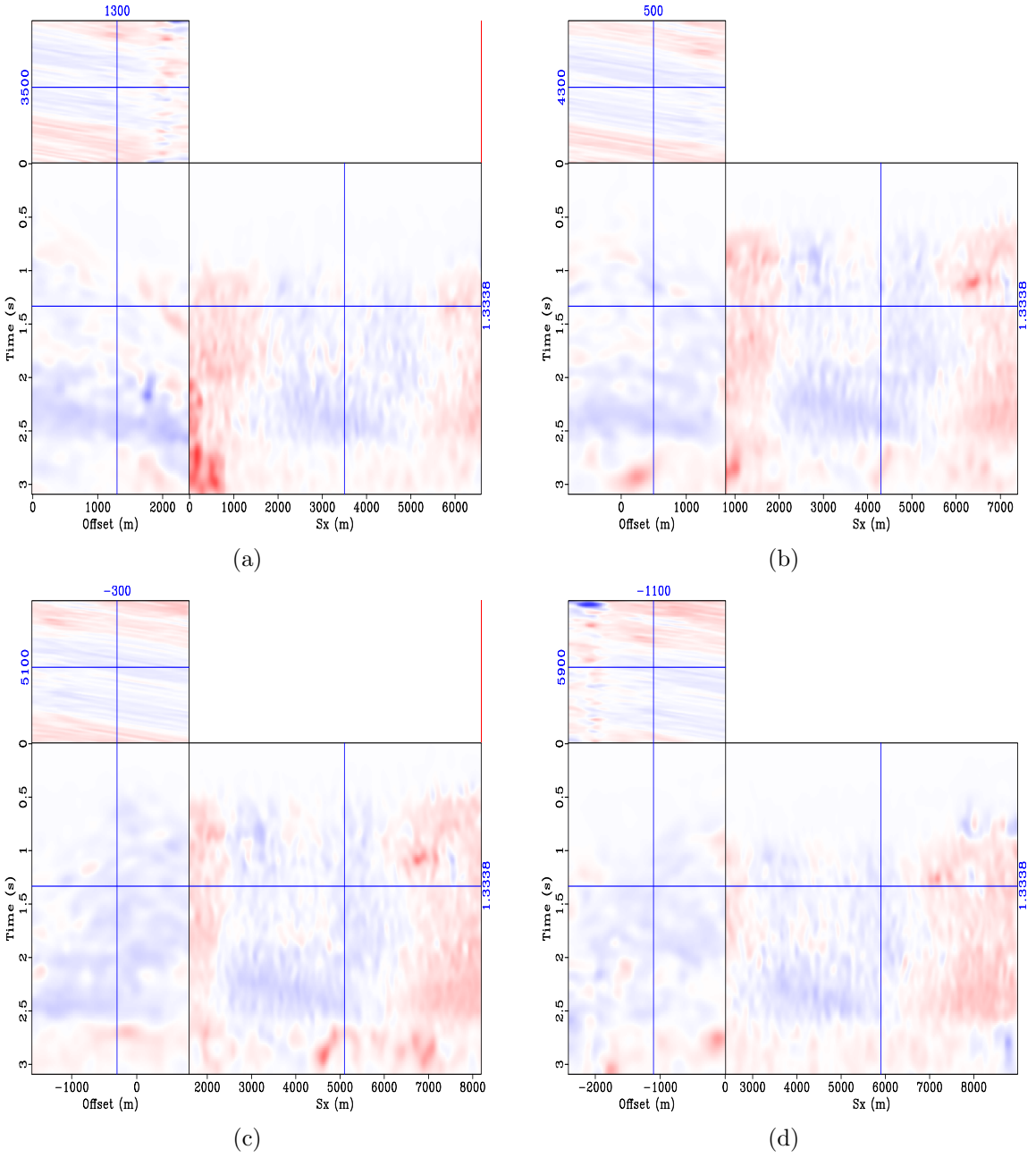

Figure 12: Local dips (common-offset components) for (a) source 1, (b) source 2, (c) source 3, and (d) source 4, obtained from the unconstrained sparse inversion (Figure 10) and used in DCSI to obtain the results in Figure 11. [**CR**]

straints are shown in Figure 15. Note the presence of several artifacts in the difference data computed from the retrieved data sets (Figures 15(e) and 15(f)). Separation results obtained by joint-inversion with spatio-temporal regularization (equation 7) are shown in Figure 16. Note that the STCSI results are cleaner than the unconstrained results. Also, note that residual artifacts present in the unconstrained difference data sets (Figures 15(e) and 15(f)) have been attenuated in the dip-constrained results (Figures 16(e) and 16(f)). Dips estimated from the unconstrained results and used to obtain the constrained results are shown in Figure 17.

DISCUSSION

Any reliable separation method for simultaneous-source data sets must be applicable to any kind of seismic data, must be independent of the number of seismic sources, and must retain important amplitude information. In the first example, we showed that our inversion formulation (DCSI) can be used to separate data from complex (sub-salt) geological environments. The separation results in Figure 4 show that l_2 inversion is inadequate for data separation. Significant improvement is obtained in the quality of these results by using a *hybrid* instead of the l_2 norm (Figure 5). In addition, the separation results can be further improved by dip-constrained inversion (Figure 6) to produce results of comparable quality to the original single-source data (Figure 3). In the second example, we showed that with our approach, we can separate any number of seismic sources. Whereas the unconstrained results (Figure 10) contain several residual artifacts, the dip-constrained results (Figure 11) are comparable to the reference single-source data (Figure 9). In the last example, we showed that this method can be applied to amplitude-sensitive studies such as time-lapse seismic reservoir monitoring. This repeatability test, shows that our method can be used to regularize and cross-equalize time-lapse simultaneous-source data sets. By incorporating both spatial and temporal constraints into the inversion, we are able to attenuate differences caused by non-repeatable acquisition parameters during the separation problem. The residual artifacts present in separately inverted data sets (Figure 15) are removed by our STCSI formulation (Figure 16).

CONCLUSIONS

We have demonstrated that simultaneous-source data sets can be separated using an inversion formulation. As shown in the numerical examples from realistic 2D models, our method can be applied in very complex geological environments, to data from multiple seismic sources and to simultaneous-source time-lapse seismic data sets. Incorporating dip information in the inversion procedure through non-stationary directional Laplacians (and in the time-lapse case, temporal constraints) helps to attenuate residual artifacts from the separation process.

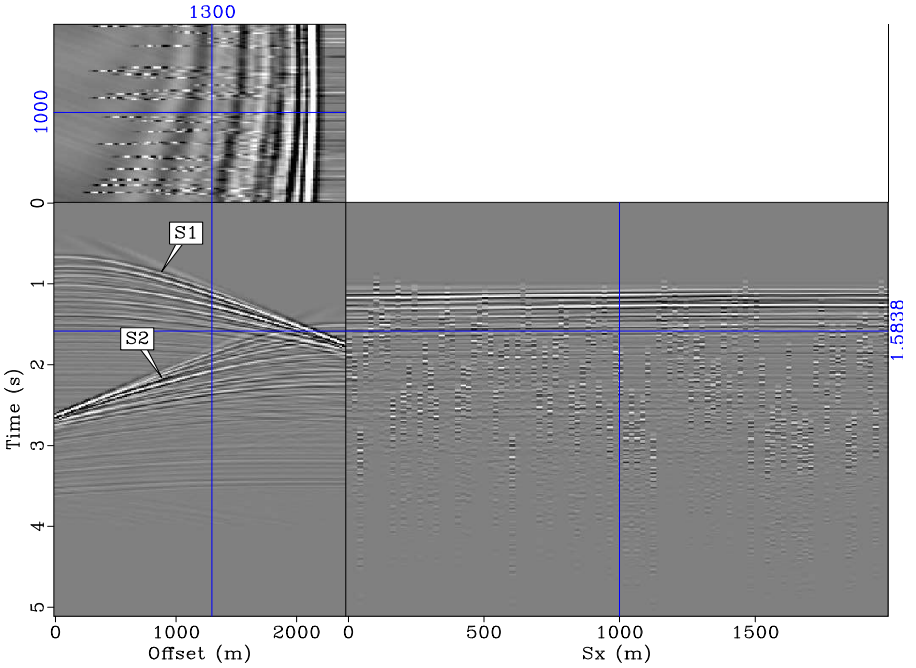

(a)

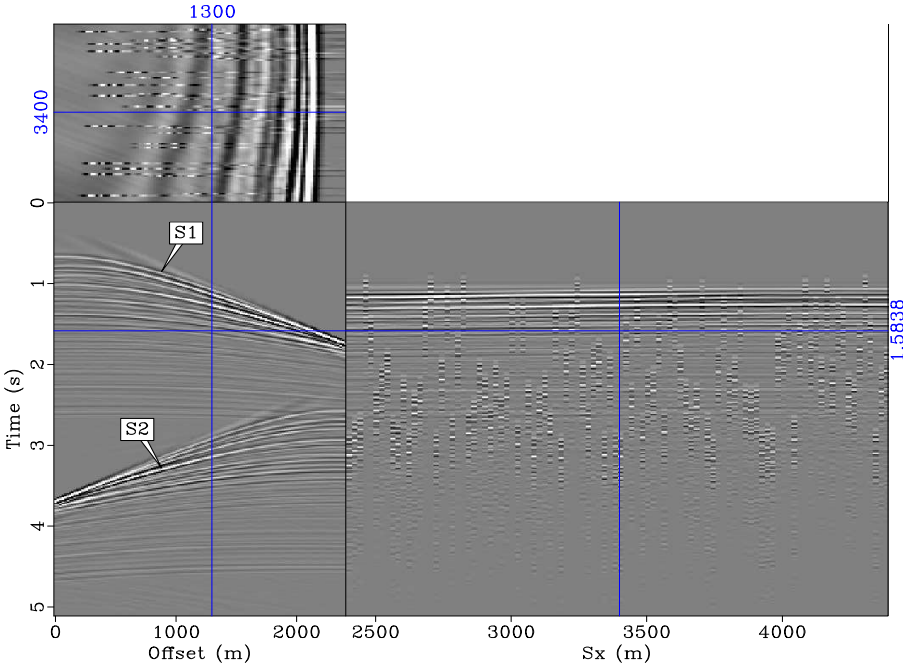

(b)

Figure 13: Simultaneous-source data sets comprising shot-records from two sources (S1 and S2) over a segment of the model in Figure 1(b). Note that the survey parameters in (a) survey 1 are different from those of (b) survey two. If not taken into account, this discrepancy (non-repeatability) will affect the quality of the time-lapse (difference) data and the resulting estimate of reservoir property change. [**CR**]

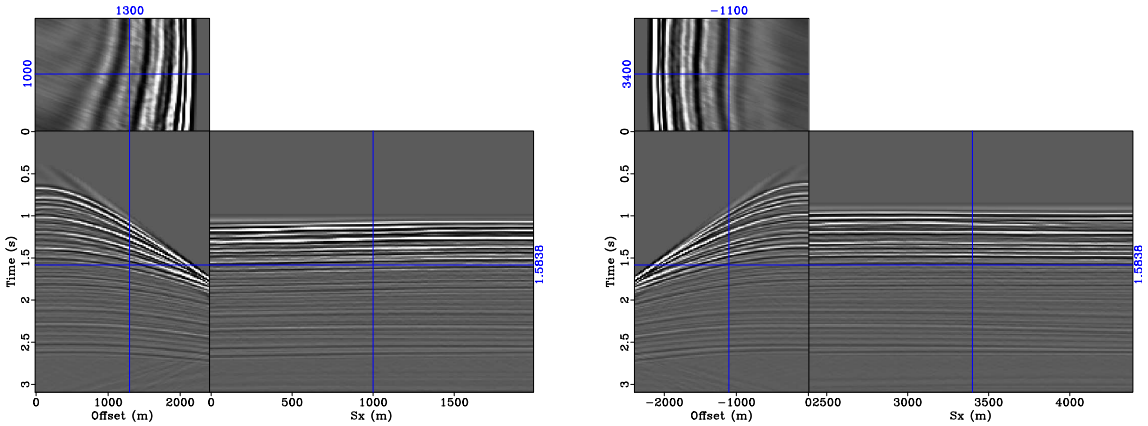

(a)

(b)

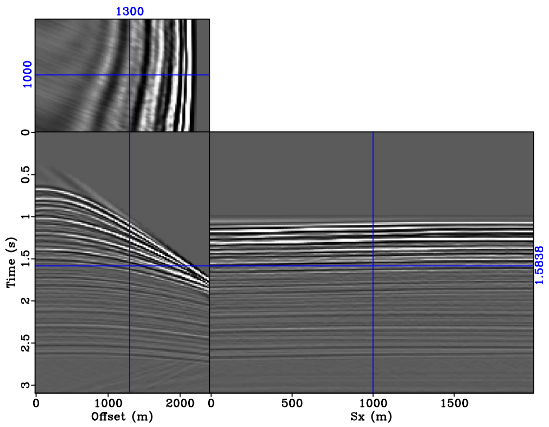

(c)

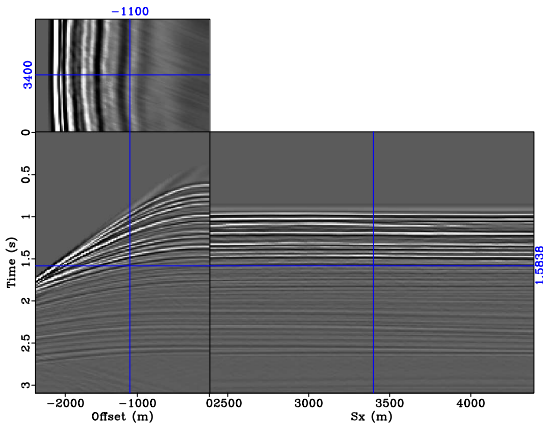

(d)

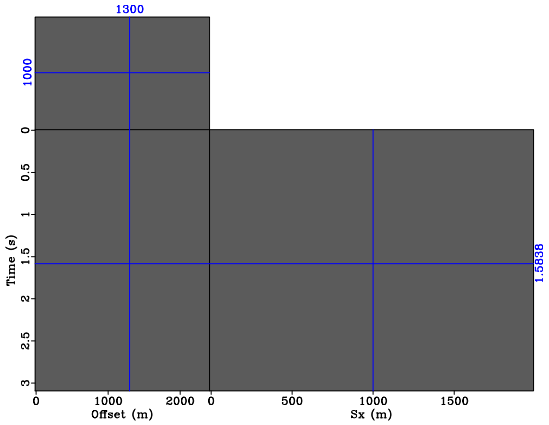

(e)

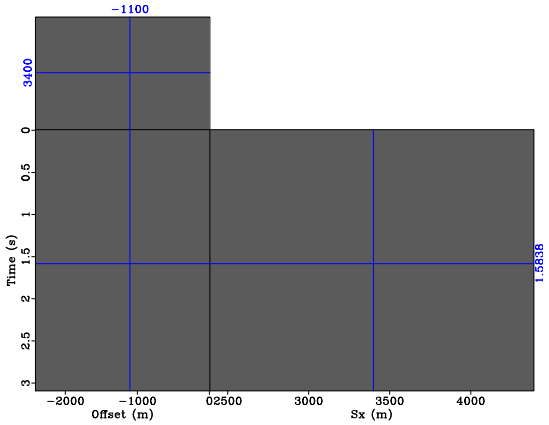

(f)

Figure 14: Single-source data that would have been recorded for (a & b) survey 1, and (c & d) survey 2 over a segment of the model in Figure 1(a); and the difference between the two surveys (e & f). The left panel represents data from source 1, whereas the right panel represents source 2. These shot records (a - d) are the components of the two data sets shown in Figure 13. Note that because there is no production-related change between the surveys, the bottom panels are blank. [**CR**]

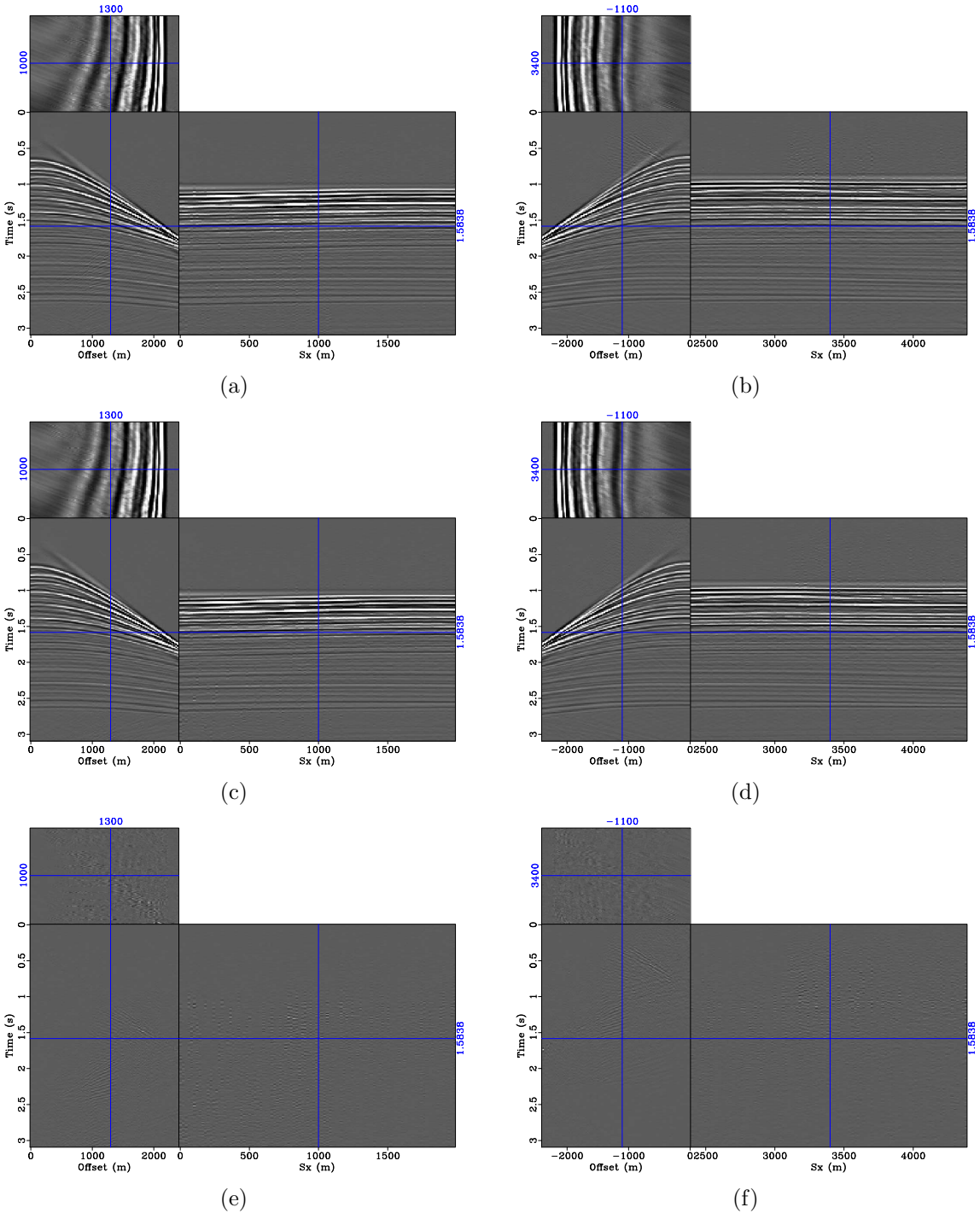

Figure 15: Shot gathers recovered by independent sparse inversion for (a & b) survey 1, and (c & d) survey 2; and the difference between the two surveys (e & f). The left panel represents data from source 1, whereas the right panel represents source 2. Note that the recovered data from the two surveys (top and middle panels) contain several artifacts. Also, note that due to the non-repeatability of the two surveys, the difference data (bottom panels) contain several artifacts. [**CR**]

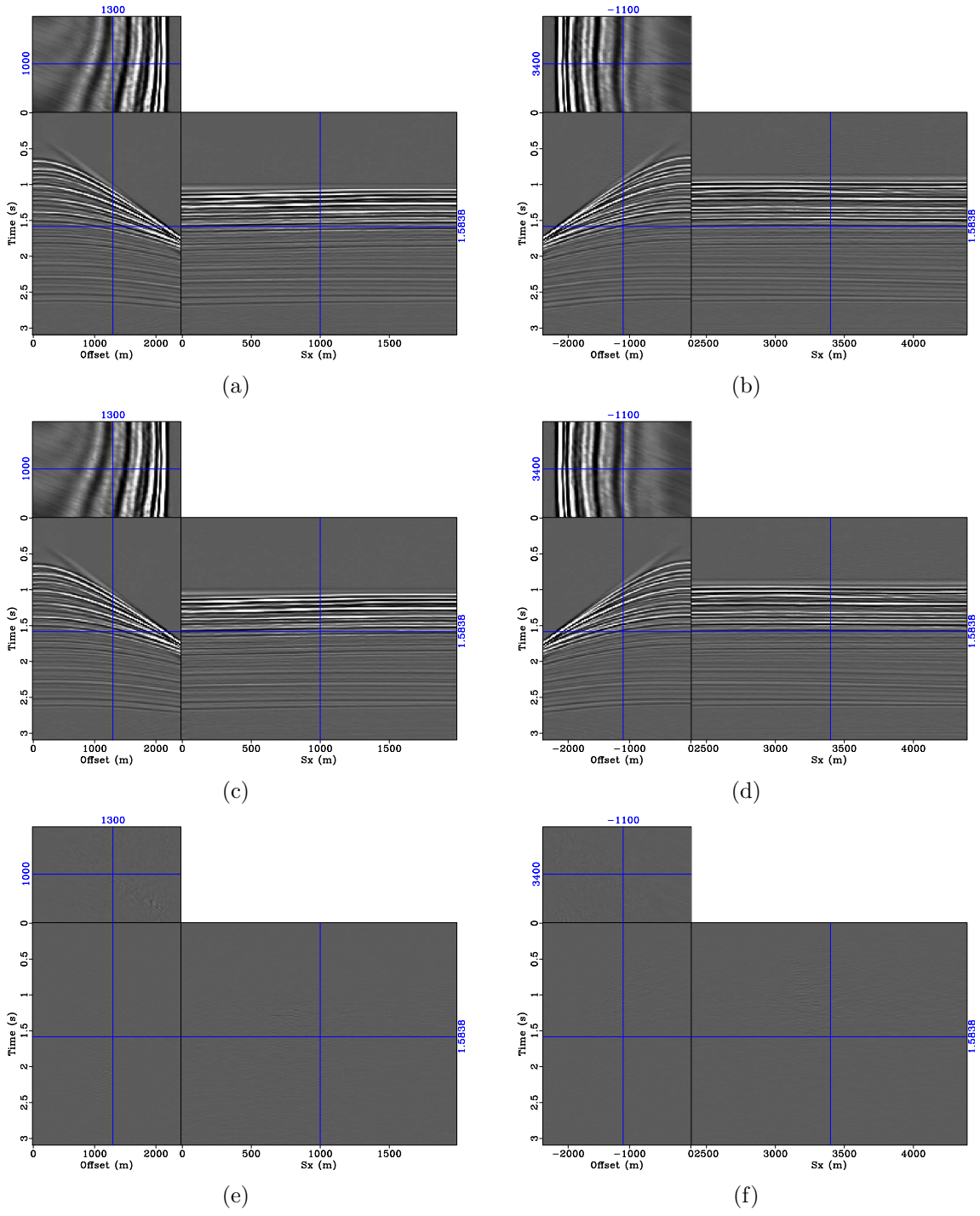

Figure 16: Shot gathers recovered by spatio-temporal constrained sparse inversion for (a & b) survey 1, and (c & d) survey 2; and the difference between the two surveys (e & f). The left panel represents data from source 1, whereas the right panel represents source 2. Note that the residual artifacts present in the unconstrained inversion results, in both the separated and difference data (Figure 15), have been attenuated by STCSI. [**CR**]

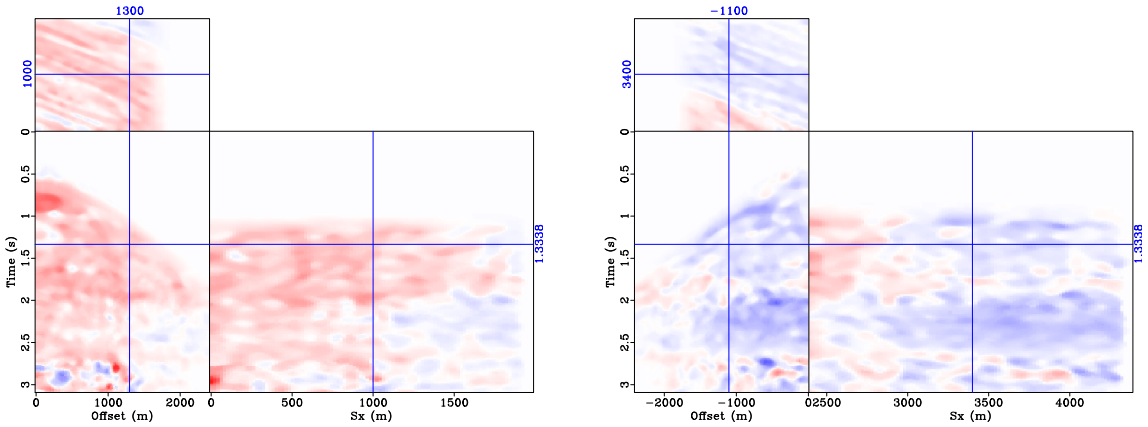

(a) (b)

Figure 17: Local dips (common-offset components) for (a) source 1 and (b) source 2 obtained from unconstrained inversion results (Figure 15), and used to obtain the STCSI results (Figure 16). Because there was no change between surveys, each panel was computed as the average of the local dip estimates for the two surveys. [**CR**]

REFERENCES

Abma, R., T. Manning, M. Tanis, J. Yu, and M. Foster, 2010, High quality separation of simultaneous sources by sparse inversion: EAGE Expanded Abstracts.

Akerberg, P., G. Hampson, J. Rickett, H. Martin, and J. Cole, 2008, Simultaneous source separation by sparse Radon transform: SEG Technical Program Expanded Abstracts, **27**, 2801–2805.

Ayeni, G., Y. Tang, and B. Biondi, 2009, Joint preconditioned least-squares inversion of simultaneous source time-lapse seismic data sets: SEG Technical Program Expanded Abstracts, **28**, 3914–3918.

Beasley, C. J., 2008, Simultaneous sources: A technology whose time has come: SEG Technical Program Expanded Abstracts, **27**, 2796–2800.

Berkhout, A. J. G., G. Blacquière, and E. Verschuur, 2008, From simultaneous shooting to blended acquisition: SEG Technical Program Expanded Abstracts, **27**, 2831–2838.

Claerbout, J. F. and S. Fomel, 2008, Image estimation by example: Geophysical soundings image construction: multidimensional autoregression.

Dai, W. and J. Schuster, 2009, Least-squares migration of simultaneous sources data with a deblurring filter: SEG Technical Program Expanded Abstracts, **28**, 2990–2994.

Fomel, S., 2002, Applications of plane-wave destruction filters: Geophysics, **67**, 1946–1960.

Hale, D., 2007, Local dip filtering with directional Laplacians: CWP Project Reiew, **567**, 91–102.

Hampson, G., J. Stefani, and F. Herkenhoff, 2008, Acquisition using simultaneous sources: SEG Technical Program Expanded Abstracts, **27**, 2816–2820.

Howe, D., M. Foster, T. Allen, I. Jack, D. Buddery, A. Choi, R. Abma, T. Manning, and M. Pfister, 2009, Independent simultaneous sweeping in Libya—full scale implementation and new developments: SEG Technical Program Expanded Abstracts, **28**, 109–111.

Huo, S., Y. Luo, and P. Kelamis, 2009, Simultaneous sources separation via multidirectional vector-median filter: SEG Technical Program Expanded Abstracts, **28**, 31–35.

Li, Y., Y. Zhang, and J. Claerbout, 2010, Geophysical applications of a novel and robust L1 solver: SEP Report, **140**.

Moore, I., B. Dragoset, T. Ommundsen, D. Wilson, C. Ward, and D. Eke, 2008, Simultaneous source separation using dithered sources: SEG Technical Program Expanded Abstracts, **27**, 2806–2810.

Tang, Y. and B. Biondi, 2009, Least-squares migration/inversion of blended data: SEG Technical Program Expanded Abstracts, **28**, 2859–2863.

van Mastrigt, P., S. Vaage, M. Dunn, and B. Pramik, 2002, Improvements in 3-d marine acquisition using continuous long offset (clo): The Leading Edge, **21**, 394–399.

Womack, J. E., J. R. Cruz, H. K. Rigdon, and G. M. Hoover, 1990, Encoding techniques for multiple source point seismic data acquisition: Geophysics, **55**, 1389–1396.